Accepted for publication in PASP

Deep Astrometric Standards (DAS) and Galactic Structure

Imants Platais, Rosemary F. G. Wyse

Department of Physics and Astronomy, Johns Hopkins University, Baltimore, MD 21218

imants,wyse@pha.jhu.edu

and

Norbert Zacharias

U.S. Naval Observatory, 3450 Mass. Ave. NW, Washington DC 20392

nz@usno.navy.mil

ABSTRACT

The advent of next-generation imaging telescopes such as LSST and Pan-STARRS has revitalized the need for deep and precise reference frames. The proposed weak-lensing observations with these facilities put the highest demands on image quality over wide angles on the sky. It is particularly difficult to achieve a sub-arcsecond PSF on stacked images, where precise astrometry plays a key role. Current astrometric standards are insufficient to achieve the science goals of these facilities. We thus propose the establishing of a few selected deep (V=25) astrometric standards (DAS). These will enable a reliable geometric calibration of solid-state mosaic detectors in the focal plane of large ground-based telescopes and make a substantial contribution to our understanding of stellar populations in the Milky Way. In this paper we motivate the need for such standards and discuss the strategy of their selection and acquisition and reduction techniques. The feasibility of DAS is demonstrated by a pilot study around the open cluster NGC 188, using the KPNO 4m CCD Mosaic camera, and by Subaru Suprime-Cam observations. The goal of reaching an accuracy of 5-10 mas in positions and obtaining absolute proper motions good to 2 mas yr^{-1} over a several square-degree area is challenging, but reachable with the NOAO 4m telescopes and CCD mosaic imagers or a similar set-up. Our proposed DAS aims to establish four fields near the Galactic plane, at widely separated coordinates. In addition

to their utilitarian purpose for DAS, the data we will obtain in these fields will enable fundamental Galactic science in their own right. The positions, proper motions, and VI photometry of faint stars will address outstanding questions of Galactic disk formation and evolution, stellar buildup and mass assembly via merger events.

Subject headings: Astrometry: general — Galaxy: structure — Solar system: KBOs

1. Introduction

Searches for the answers to fundamental questions of astrophysics and cosmology have often resulted in technological challenges and advances. The drive to understand the nature of dark matter and dark energy has led to proposals for ground-based telescopes with large étendue (the product of aperture, A, and field-of-view, Ω), reaching as high as 250 m^2 deg^2. Such systems enable deep, high-cadence and throughput, multi-band imaging of the visible sky up to 3π steradians in area – crucial not only to studies in cosmology but also of supernovae, faint optical transients, and small bodies in the Solar system.

The success of large digital sky surveys such as 2MASS and SDSS has shown we can cope with large dataflows and databases, and pointed to necessary future developments, while recent advances in complex detector designs (Groom 2000), have made ever-larger focal plane arrays feasible. The most advanced facilities, in terms of their actual implementation, are the Pan-STARRS (Kaiser 2004; Hodapp et al. 2004) array of 1.8m wide-field telescopes and the 8.4m Large Synoptic Survey Telescope (Claver et al. 2004) (LSST). A distinctive feature of each of these observatories is a large field-of-view (7-10 deg^2), achieved by applying an innovative optical design in combination with a huge 1-3 Gpixel camera, in which the focal plane is close-packed with several hundred solid-state detectors, e.g., CCD chips forming a Focal Plane Array (FPA). Each detector, however, is an autonomous unit with its own characteristics. In order to emulate a single unified detector, the parameters of each individual unit, including its exact location and geometric distortions introduced by the optics, must be calibrated.

These calibrations are crucial at least in two major applications: i) image resampling and stacking and ii) wide-field astrometry (positions and proper motions). Both of them are *critical* for weak lens tomography and the requirement to reach 10σ limiting magnitude of $V = 28$ by co-adding dithered images (Tyson 2002). The coherent galaxy shape distortions caused by cosmological weak lensing do not exceed 1-2% changes in the ellipticity (a weighted

central second moment) of galaxy images (cf. Van Waerbeke et al. (2000)). If we assume the average apparent size of faint galaxies to be $\sim 3''$, then the lensing signal is only on the order of 30 mas or less. Such a small signal can be easily confused with systematic errors originating from imperfect knowledge of the PSF shape, or from inadequate correction for geometric distortions in dithered images. Thus, translating the acceptable tolerances in the quality of the PSF, the LSST Focal Plane Array should be calibrated geometrically to a precision of $\sim 0.5\,\mu$m or better, corresponding to ~ 10 mas on the sky. Measurements of such high precision are not possible to perform in the laboratory, and therefore the FPA should be calibrated and monitored astrometrically on the telescope, using star images as fiducial points of reference. If accurate celestial coordinates of such stars are not known, self-calibration techniques (Anderson & King 2003) can, in principle, provide a provisional reference frame, albeit with an arbitrary scale and orientation. However, the presence of geometric distortions and a 'broken' (discontinuous) FPA would require on the order of a hundred optimally dithered, overlapping, and rotated frames, to assure the success of self-calibration. Further, high level of instrumental and atmospheric stability is essential while continuously obtaining the necessary sequences of such images.

In contrast, all that is needed to calibrate any FPA is a few exposures of a dense, deep, and externally accurate astrometric standard or reference frame. Once derived, the calibration constants are valid over prolonged periods of time, and can be monitored by re-observing regularly the same astrometric standard. Only such astrometrically flattened frames can then be shifted and co-added without a loss of precision.

In this paper we describe the status of existing astrometric reference frames and show that there is a pressing need to set up a few new deep astrometric standards specifically for the needs of large imaging telescopes. The range of magnitudes of the existing high-accuracy astrometric standards are too bright for the optimal range of LSST or other facilities with a similar étendue. In just 10 s of integration time, LSST reaches $V = 24$ and saturates everything brighter than $V \sim 17$ (Tyson 2002). Further difficulties arise from the fact that short exposures are affected substantially by atmospheric noise, which diminishes only over a longer 30-60 s integration time. With these longer integrations, the saturation level would drop to even fainter magnitudes.

We argue that deep astrometric standards (DAS), together with elements of the self-calibrating techniques, will then enable the calibration of the FPA to the required precision level. The DAS fields can be observed and completed on the timescale of a few years, significantly prior to the launch (June 2011) and subsequent catalog release at mission end (yr. 2020) from GAIA. Absolute proper motions are an important aspect of these astrometric standards, and these will provide essential constraints on stellar kinematics and Galactic

structure models. At present, transverse kinematic data over significant parts of the sky are available down to $V \sim 18$ with proper motion accuracies not better than ~ 6 mas yr^{-1} (Hanson et al. 2004; Girard et al. 2004). Two deeper ($B \sim 22$) proper motion studies (Chiu 1980; Majewski 1992), with proper motion accuracies of around 1 mas yr^{-1} or better, probe only a small area in a few lines of sight at high Galactic latitude. It is fair to say that we do not know the kinematics of Galactic populations fainter than $V \sim 21$, especially near the Galactic plane. For operational reasons, the selection of potential astrometric standards is limited to low Galactic latitudes, motivated by the need to have a high surface density of stars over the sky. Thus, the astrometric standards are expected to make a substantial contribution in constraining Galactic structure models via very deep starcounts, multicolor photometry and proper motions, with an emphasis on the thick and thin disks.

A favorable combination of pressing calibration needs for large imaging facilities, unsolved issues of Galactic structure, and availability of the appropriate instruments makes the idea of deep astrometric standards both feasible and timely. We discuss here in some detail all the required steps in establishing such standards.

2. Celestial Reference Frames

2.1. Primary reference frames

At a fundamental level, the International Celestial Reference System (ICRS) defines the coordinate axes, and is established by the VLBI positions of 212 defining compact extragalactic radio sources. A set of these and additional 505 sources currently constitutes the International Celestial Reference Frame (ICRF) – the most accurate (source positional errors at a 0.25 mas level and the frame orientation good to 20 μas), albeit very sparse, reference frame (Ma et al. 1998; Fey et al. 2004). At optical wavelengths the ICRS is represented by the Hipparcos Celestial Reference Frame (HCRF) determined by the Hipparcos Catalogue (ESA 1997), excluding all stars flagged as known, and suspected binary and multiple systems. The accuracy of the HCRF is steadily deteriorating, mainly due to accumulating positional errors from the errors in proper motions of the stars, and, by 2006, a typical Hipparcos star will have a ~ 15 mas error in its position. Furthermore, the low density of Hipparcos stars (on average three stars per deg^2) and their high brightness ($V \lesssim 10$) prevents direct use of Hipparcos stars as a reference frame in most applications.

The Tycho-2 catalog (Høg et al. 2000), containing positions and proper motions for the 2.5 million brightest stars in the sky, provides a denser reference frame. The average density of Tycho-2 stars per deg^2 ranges from 20 to 150, depending upon the Galactic latitude. By

2006, the typical positional errors of Tycho-2 stars will be at the level of 15 to 100 mas, with the larger errors corresponding to the Tycho-2 limiting magnitude at $V \sim 12$.

The second US Naval Observatory CCD Astrograph Catalog (UCAC) provides a dense and accurate reference frame based on Tycho-2 and, hence, indirectly on HCRF (Zacharias et al. 2004). Down to its limiting magnitude at $r_{\rm UCAC} \sim 16$ this catalog yields a factor of ~ 30 more stars per deg^2 than does Tycho-2, and surpasses the precision of Tycho-2 at $V \sim 10$ and fainter. The precision of UCAC positions is 15-70 mas, depending on magnitude. Owing to a number of innovations and the astrometry-driven approch to all stages of the observations and reductions (Zacharias et al. 2000, 2004), the UCAC currently is the premier source of reference stars at optical wavelengths.

2.2. Future reference frames

For large telescopes, direct use of any of the reference frames listed above would be problematic, due to the required shortness of the exposures to avoid saturation, and due to the relatively low surface density of reference stars, thus limiting their number accessible in any one of the CCD detectors in the FPA. There are four large programs which are designed to improve the reference frame, from substantially to dramatically, and extend it down to $V \sim 20$.

2.2.1. URAT

The USNO Robotic Astrometric Telescope (URAT) is the next step in the quest for an ever-fainter, denser, and more precise reference frame (Zacharias 2004a). This is a 0.9m astrometric telescope of innovative design and is intended to provide all-sky reference stars at a 5-10 mas accuracy level, and with about 30 mas errors at the limiting magnitude $r_{\rm URAT} \sim 20$. The proposed link of the URAT coordinates directly to ICRF, in combination with block-adjustment reduction techniques, (Zacharias 1992) not only will improve the alignment of the optical frame but will also provide a much needed zeropoint for absolute trigonometric parallaxes. The expected time frame of the URAT catalog release is 2010.

2.2.2. Space missions: GAIA, OBSS, and SIM

It is commonly acknowledged that the Hipparcos mission revolutionized astrometry. At the time, however, the existing technology limited the depth of the survey and the number

of available targets to about 120,000, and necessitated an input catalog, as opposed to a true survey. The next generation ESA cornerstone mission GAIA (Perryman 2002) takes advantage of many techological advancements and is designed to obtain very precise positions and other astrometric parameters down to $V \sim 20$ for one billion objects all over the sky. It should provide a reference frame at a micro-arc-second (μas) level, that is by about two orders of magnitude better than is currently possible from the ground at optical wavelengths. The first early data release from GAIA is not expected before 2014, with the final catalog release at mission-end, around 2020.

The Origins Billion Star Survey – OBSS (Johnston et al. 2004) is one of the proposals selected by NASA for study within its Astronomical Search for Origins program. The OBSS mission has similar goals to GAIA, but considers a different observing strategy and has flexibility in the selected fields to observe down to $V = 25$. If approved for flight, this mission is likely to be scheduled for the post-GAIA timeframe.

The NASA Space Interferometry Mission (now the rescoped SIM PlanetQuest) has multiple scientific goals, ranging from searches for extrasolar planets to probing the astrophysics of QSOs. It will also provide a global astrometric grid at a few μas accuracy level and similar precision wide-angle astrometry for $\sim 20,000$ pre-selected stars (Marr 2003).

2.3. Secondary reference frames

The 20th century's monumental efforts to image the sky has lead to numerous deep photographic surveys in various bandpasses, now digitized and reduced into catalogs of objects. The most advanced, in astrometric terms, in this class is the three-color, two-epoch catalog USNO-B1.0 (Monet et al. 2003) which provides reference stars down to $V \sim 21$ with 200 mas accuracy at J2000. As noted by Monet et al. (2003), while this catalog represents a milestone in the processing of the object detection archive, more (planned) calibrations and verifications are required for full exploitation of its astrometric potential.

The 2MASS near-infrared All-Sky Catalog of Point Sources (Cutri et al. 2003), complete down to $J = 15.8$ and yielding 70 mas positional accuracy at the epochs 1997-2001 – the span of 2MASS observations – is a very useful source of positions. Similarly, the Sloan Digitized Sky Survey (SDSS) provides wide-area, one-epoch zonal catalogs accurate to 45 mas down to $r \sim 20$, and to 100 mas at $r \sim 22$ (Pier et al. 2003). Such catalogs, though, cannot be considered as true secondary reference frames since the lack of proper motions makes it impossible to extrapolate the positions to an arbitrary epoch. Therefore, the US Naval Observatory has launched an initiative to combine various sources of astrometric

and photometric data into the Naval Observatory Merged Astrometric Dataset (NOMAD, Zacharias et al. (2004b)). One of the goals of this program is to minimize local and global systematic errors.

2.4. Astrometric potential of deep surveys

As shown above, the limiting magnitude of reference stars with good existing astrometry is only about $V = 15$, with possible planned extensions to $V \sim 20$. Only larger (4m) aperture telescopes and longer exposure times ($t_{exp} \gtrsim 10$ min) will allow us to probe several magnitudes deeper. There are at least four deep optical surveys which reach $V \sim 25$ and cover several deg^2 on the sky: the NOAO Deep Wide-Field Survey (Jannuzi et al. 2004), the CFHT12K-VIRMOS survey (Le Fèvre et al. 2004), the CFHT Legacy Survey (Veillet et al. 2001), and the Deep Lens Survey (Wittman et al. 2002). Essentially all of these surveys are tailored to study various aspects of external galaxies, large scale structures, and cosmology. As a result, the selected fields are located at high Galactic latitudes in order to minimize the "contamination" by intervening Milky Way stars and Galactic interstellar extinction. This kind of minimization, however, is detrimental to astrometry, since astrometric precision is roughly proportional to $1/\sqrt{n}$, where n is the number of reference stars. Star-count models (e.g. Gilmore (1981); Robin et al. (2003)) predict that the cumulative number of stars at high Galactic latitudes ($b \gtrsim 45°$) and with $V < 20$ is only about 1,000-2,000 stars per deg^2.

One survey which does get close to the Galactic plane is the CFHTLS Very Wide Shallow survey of the ecliptic (Veillet et al. 2001). Having multiple epoch observations in the Sloan g', r', i' filters, it has a potential to provide accurate positions down to about $V = 23$ at low Galactic latitudes, lines-of-sight that are abundant with stars. Since this survey is fine-tuned for Kuiper Belt Object (KBO) searches and follow-up, the realization of its full astrometric potential is uncertain.

3. Deep Astrometric Standards (DAS)

The basic astrometric parameters of any celestial object are the position and motion in the adopted reference system and a parallactic displacement. Astrometry in essence is a relentless process of establishing better and denser reference frames so that these basic parameters can be determined with ever increasing accuracy. As shown in the previous section, the existing or the near future reference frames do not extend significantly beyond

$V \sim 20$, and in certain applications such as imaging with LSST, that is a serious limitation.

3.1. A rationale for DAS: astrometry and science case

To provide special astrometric support for large optical imaging facilities, we propose the Deep Astrometric Standard (DAS) initiative. In accordance with the projected specifications of these facilities and the technical capabilities of ground-based, 4m class imaging telescopes, the DAS are designed to provide high-precision positions and photometry over selected circular 10-deg^2 areas down to $V = 25$. These standards will serve as primary reference coordinate sets to calibrate the Focal Plane Assembly unit for any large-aperture telescope and to enable positional stability monitoring of the individual units of the FPA – solid-state detectors such as CCD and CMOS. The accuracy of DAS is limited by the accuracy of the primary reference frames at optical wavelengths, i.e. at the level of 5-10 mas, but this will be improved each time a better global reference frame becomes available, e.g., URAT, GAIA.

In accordance with the mandatory operational requirements described in the following section, the DAS fields are selected towards the Galactic anticenter and inner disk. The photometry and proper motions as deep as $V = 25$ in these directions should provide new insights into Galactic structure and galaxy evolution. Towards the anticenter it will trace the edge of the disk, probe the disk flare and low-latitude stellar streams. In the direction of Sagittarius and Ophiuchus, the thick disk scale-length, the extent of bulge, and contribution by the Sagittarius dSph galaxy at faint magnitudes are a few key questions not yet fully answered. An unprecedented combination of depth and spatial coverage of the DAS fields at low Galactic latitudes is critical in attempting to decipher the complex structure of the Galaxy.

3.2. Strategy in setting up a DAS field

The current designs of large survey telescopes, e.g. (Hodapp et al. 2004), favor a semi-round FOV, with the diameter ranging between 3° to 3.°5. Thus, the upper limit of a proposed FOV is about 10 deg^2 and that is also the area we propose here for a DAS field. With the NOAO CCD mosaic imagers at 4m telescopes (FOV= $36' \times 36'$) it requires 37 partially overlapping pointings to fill in a round 10 deg^2 FOV (Fig. 1).

There are several operational requirements as to how to set up such standards optimally, considering that the majority of the world's premier large imaging facilities (existing and

planned) are located within geographic latitudes of $-35^\circ < \phi < +35^\circ$.

1. To ensure access from both hemispheres, the fields should be located near the celestial equator.

2. To ensure year-long access, there must be at least two directions containing the standard fields separated in right ascension by ~ 12 hrs.

3. To minimize the effect of atmospheric refraction, one astrometric standard must cross the meridian at a zenith distance $z \leq 20^\circ$ while another standard at a higher z serves as a back-up and a check on refraction corrections. Therefore, the optimal configuration is a pair of fields at similar right ascensions and located symmetrically to within $\pm 20^\circ$ on both sides from the equator.

4. A field must be dominated by stars, not galaxies which cannot be centered as precisely as can stars. Hence, the fields should be near the Galactic equator as well. Note that the celestial and Galactic equators cross each other at RA=$6\overset{\mathrm{h}}{.}86$ and $18\overset{\mathrm{h}}{.}86$ (J2000).

5. A field must be free of dark clouds or emission nebulae and should not contain bright stars ($V \lesssim 7$). A fairly uniform and not-too-dense distribution of stars across the field is also required. The POSS photographic atlas is convenient in searches for promising directions on the sky. Similarly, the Hipparcos Millennium star atlas is useful in locating areas devoid of bright stars.

3.3. First DAS fields

Guided by the criteria outlined in Sect 3.2 and by the desire to maximize the science return, we made a selection of four DAS fields (Table 1). There are two Northern 'winter' fields (GTO, Hya) and two 'summer' fields – Oph and Sgr. Thus, for each hemisphere there are two primary and two secondary astrometric standard fields. A visibility analysis for the KPNO and CTIO locations indicates two one-month windows when no primary standard field is culminating at night, but that alone does not warrant setting up additional fields far away from the equator. Two fields cross the ecliptic plane, where searches for Kuiper Belt Objects are feasible. One of the toughest requirements is avoiding bright stars in a 10 deg^2 field. In the selected DAS fields the brightest star is at $V = 6.4$. It should be noted that our minimalistic approach to the selection of fields is dictated by telescope time limitations. More deep fields in other directions would provide more constraints to Galactic models and would also ease the astrometric calibrations.

From the standpoint of interstellar extinction three of our DAS fields are almost transparent. The mean reddening $E(B-V)$ values are obtained from Schlegel, Finkbeiner & Davis (1998) maps. The GOT (Gemini-Orion-Taurus) field has a much higher mean reddening, namely, $E(B-V) \sim 1.4$ which amounts to ~ 4.5 mag of a total absorption in the V bandpass. This field (see Mermilliod (1998)) contains three sparse open clusters having the following reddening and distance: NGC 2129 ($E(B-V)$=0.6; d=1.5 kpc), Berk 21 ($E(B-V)$=0.7; d=5.0 kpc) and Basel 11b ($E(B-V)$=0.3; d=1.7 kpc), thus indicating that the light absorbing material is not distributed evenly and there very well could be windows with lower absorption.

Star-count models are most reliable away from the Galactic plane, where extinction is lower and the stellar distribution is smoother. The Besançon model adopts a different approach, one of stellar population synthesis (Robin et al. 2003). We obtained the expected number of stars per deg^2 in our proposed fields using both a straightforward star-count model (Gilmore 1981) and the Besançon population synthesis model. These are indicated by the last two columns in Table 1, where good agreement is seen apart from close to the disk plane. Guided by these apparent stellar densities it may appear that crowding could be severe. Therefore in November 2004 we obtained a series of VI exposures in the GOT field ranging from 10 s to 900 s with the NOAO 4m telescope and CCD mosaic imager (FOV=0.36 deg^2). From the long exposures, the average number of unsaturated and well-centered images (centroid $\sigma \sim 0.05$ pix) over the entire CCD mosaic is 16,000 or well below the acceptable level of crowding. Extrapolating smoothly over the entire 10 deg^2 leads to an expected total number of stars down to V=25 in the GOT field of $\sim 500,000$. This is significantly lower than the model predictions. A trial 10 min exposure of the Sgr field in the V bandpass indicated $\sim 60,000$ stellar images over the entire CCD mosaic and no substantial crowding across the field. This high a number of stars with precise positions should provide an excellent reference frame to support astrometric calibration of any CCD mosaic in existence or in the planning stages. Despite the preliminary status of the measured stellar densities, we note large discrepancies between the model predictions themselves and between either model and the actual starcounts. The DAS program is well-suited to resolve these differences towards the selected directions, although it is clearly not optimal for the entire Galaxy due to the small number of fields.

The Galactic coordinates of the selected fields show that the Oph and Sgr fields probe the Galactic inner disk, while the GOT field is close to the Galactic anticenter, and the Hya field is closer to the direction of Galactic rotation. It is instructive to review what these directions can offer for studies of Galactic structure and kinematics.

3.4. Galactic structure studies with DAS fields

These astrometric standard fields are expected to make a substantial contribution to constraining Galactic structure models and our understanding of the Milky Way stellar populations. Each of the four fields contributes to a specific aspect, and taken all together will provide constraints on population gradients and substructures. Our individual fields are large enough to probe gradients on $\sim$ kpc scale – at a fiducial distance of 10 kpc ($V = 20$ and $M_V = +5$), three degrees on the sky corresponds to $\sim$ 500 pc – and more distant stars probe even larger spatial extent. The deep photometric data will allow star-count analyses, e.g., Siegel et al. (2002) to constrain the particularly poorly known radial distributions of the thick and thin disks. The depth of these fields at $V = 25$ would allow the detection of G-dwarfs ($M_V = +5$) out to 100 kpc, with no extinction, and out to 16 kpc in the more heavily reddened GOT field. Even more importantly, the accuracy of our DAS absolute proper motions is expected to be $\sim$ 2 mas/yr, a factor of three better than the quoted rms error of the photographic-based Lick proper motion catalog (Hanson et al. 2004), and only a factor of two below the 4-m (photographic) survey of Majewski (1992) which used a 16 year baseline and which was limited to $B \sim 22.5$, some 1.5 magnitudes brighter than our limiting magnitude. Our data will provide the deepest available absolute proper motion data over relatively large areas of the sky. They will enable diverse science projects such as refining the kinematical properties of Galactic stellar populations (Majewski 1992; Mendez et al. 2000), identification of debris from Galactic mergers (Majewski, Munn & Hawley 1996), and constraints on the surface mass density of the disk. The Reduced Proper Motion Diagram (RPMD) would provide nearly distance-independent classification of Galactic populations that incorporates kinematics. Stars can be classified by their location on this diagram (e.g. Salim & Gould (2002)), greatly facilitating the identification and characterization of Galactic stellar components, such as the thick disk, first kinematically identified through this technique (Wyse & Gilmore 1986), and the Galactic halo (Gould 2003). The fields will be particularly useful for investigations of the Galactic disk, which has gained new interest as both recent observations, indicating unexpected substructure (e.g., Newberg, Yanny et al. (2002)) and recent theory, indicating significant mergers into the thin disk (e.g., Abadi et al. (2003)), have emphazised our lack of knowledge of the disk far from the solar circle and its importance in constraining theories of disk galaxy formation and evolution.

At faint magnitudes, accurate star-galaxy separation is crucial to the interpretation of starcounts. As shown by Reid et al. (1996), at high galactic latitudes ($b > 45°$) the surface densities of stars and galaxies are equal at $I \sim 18.5$, and at $I \sim 24$ galaxies outnumber stars by a factor of $\sim$ 40. The DAS fields are located at low and moderate galactic latitudes, therefore the contamination ratio of galaxies is reduced by a factor 6-75 compared to high Galactic latitudes. Additionally, background galaxies tend to be bluer than low-mass disk

stars, which are the dominant contributor in our four fields. A combination of object morphology and CMD analysis is expected to provide a reliable discrimination between stars and galaxies, with proper motions greatly helping.

3.4.1. The outer edge of the Galactic disk

The GOT field is conveniently positioned to probe the outermost regions of the disk in the anti-center direction. At 8 kpc, a $3\overset{\circ}{.}5$-diameter field probes a ~ 500 pc wide spatial cone and we should therefore be able to constrain possible variations in thin-disk scale-height (i.e. flaring) in addition to determining the disk scale-length (cf. Robin et al. (1992a)) and investigating the putative disk 'edge' at ~ 6 kpc from the Sun (Robin et al. 1992b). These latter results were based on star counts to a similar depth as we propose ($V = 25$), but over a much smaller area, only 0.008 deg^2. The direction of the Galactic anticenter towards Taurus is strewn with dark nebulae and star forming regions that have a high and variable extinction. The much larger area (a factor of ~ 1000) of our survey provides an opportunity to map out extinction and find new transparency windows through which to measure the disk parameters.

3.4.2. The Stellar Warp in the Disk

Another aspect of our ignorance about the outer Galactic disk is the amplitude and shape of the warp in the stellar disk of the Milky way. Does it follow that in the gas? Do old stars and young stars exhibit different warp structure? The warp has taken on new importance recently due to the controversy about the role it could play in the overall non-axisymmetric structure in the stellar disk. There have been claims and counter claims as to whether or not the stellar warp has parameters sufficient to mimic a distinct overdensity such as has been identifed as the core of the proposed Canis Major dwarf galaxy at $\ell = 240^\circ$, $b = -7^\circ$ (Bellazzini et al. 2004; Martin et al. 2004a,b; Momany et al. 2004). Our Hya field probes the corresponding northern latitudes to these fields, where the warp should manifest itself as a lack of distant disk stars. Again, our fields are sufficiently large that we will be able to constrain the warp parameters by star counts across the field.

3.4.3. The surface mass density of the disk

Our outer disk fields can be used to facilitate the estimation of the surface mass density of the disk beyond the solar neighborhood. Disk dwarfs can be identified through the reduced proper motion diagram, and spectroscopic follow-up will allow the determination of metallicities and thus photometric parallaxes, together with full 3-D space motions. The vertical motions may then be combined with vertical star counts in an analysis of the total surface mass density in the disk (cf. Kuijken & Gilmore (1989)).

3.4.4. Substructures in disk & halo

Our Hya and GOT fields will also shed more light on the 'ring' that apparently encompasses the Galaxy (Ibata et al. 2003), seen most prominently in the anticenter direction (Newberg, Yanny et al. 2002; Yanny & Newberg et al. 2003). Is this a feature in the disk, or a remnant of a shredded galaxy, such as the Canis Major dwarf discussed above? Our large fields and widely separated lines of sight to the outer disk will constrain both small-scale and larger-scale variations, particularly when combined with imaging data from the Sloan Digital Sky Survey and its extension SEGUE (Beers et al. 2004).

Our Sgr field is located at a prominent tail from the Sagittarius dwarf spheroidal, seen clearly in M-giants (see Fig. 3 in Majewski et al. (2003)). A detailed knowledge of stellar population in the tail will better constrain models of the dynamical interaction.

Our expected proper motion error of 2 mas/yr at a distance of one kpc translates into a transverse velocity error of 10 km/s, and at distances larger than about 10 kpc, the transverse velocity error is large enough to make even statistical separation of populations by proper motions alone difficult. This problem is substantially mitigated by applying the Reduced Proper Motion Diagram, which will be used in the analysis. Indeed, our deep photometry and precise proper motions allow the derivation of reduced proper motion diagrams with low enough errors that a distance-independent identification of substructure in this plane may be carried out. We note that at our faint magnitudes, $V \gtrsim 19$, giants with absolute magnitudes $M_V \sim -1$ are at distances of greater than 100 kpc, the very outer limits of the stellar halo of the Milky Way (e.g. as traced by RR Lyrae in the Sloan Digital Sky Survey, Ivezic et al. (2004)). Our analysis will therefore be using main sequence stars, the dominant stellar populations, and probe distances from several kiloparsecs ($V \sim 19$) to the edges of the stellar halo ($V \sim 25$). One should note that kinematic signatures of substructure are not limited to the outer halo where dynamical times are longest – on the contrary, there is a wealth of local (less than 1 kpc) 'moving groups' (e.g. Famaey et al. (2005); Helmi et al. (2005))

and the challenge is to identify their origins – some clearly are better interpreted as due to dynamical perturbations in the local disk. Extending our knowledge with fainter stars, such as could be achieved with the dataset proposed here, would clearly be beneficial, albeit that our pencil-beam approach, as opposed to all-sky, provides more limited constraints. Dinescu et al. (2002) demonstrate the power of pencil-beam proper-motion surveys, with data that are shallow by the standards of the survey proposed here, but more precise.

3.4.5. Halo/bulge interface

The Oph field, and the Sgr field, probe the halo/bulge interface and the inner disk along the line-of-sight. Much recent interest concerns the nature of 'pseudo-bulges' which have exponential surface brightness profiles, rather than the canonical $R^{1/4}$ de Vaucouleurs' profile (e.g. Wyse (1999); Kormendy & Kennicutt (2004)). A possibility is that they result from long-timescale instabilities in the inner disk, associated with the formation and destruction of bars. The Milky Way bulge is apparently such a 'pseudo-bulge' and the data from our deep fields here will allow investigation of the similarity or otherwise of the stellar populations in the inner disk and bulge, necessary for such secular evolution models of bulge formation. The further decomposition of the central regions into 'halo' and 'bulge' is important in understanding formation scenarios for the Galaxy.

3.4.6. Low mass & low luminosity objects

Our wide, deep fields provide an opportunity to study rare, faint objects such as white dwarfs and L and T brown dwarfs. Due to the intrinsic faintness of L and T dwarfs it is essential to have a combination of depth, color and *kinematic* information just to identify these low-mass Galactic constituents. The same holds true for the more massive white dwarfs. The luminosity functions of each of these objects is still uncertain, at best. Scaled to the CFHT Legacy Survey estimates (Veillet et al. 2001), the DAS will be able to probe the population of L dwarfs out to ~ 250 pc. Much dimmer T dwarfs can be traced out to 30 pc. Our white dwarf candidates will be identified by their reduced proper motions, allowing spectroscopic follow-up.

3.5. Kuiper Belt objects

To maximize the science return, we may want to explore the two areas where all three planes – equatorial, Galactic, and ecliptic – get close together. Since the searches for Kuiper Belt objects (KBO) such as Deep Ecliptic Survey (Millis et al. 2002) partially avoid the Galactic plane, due the crowding and the presence of bright stars, DAS should be able to fill in this gap. In addition, DAS will go ~ 0.5 magnitudes deeper than will the Deep Ecliptic survey and will provide VI photometry for all detected KBOs. The compilation by (Hainaut & Delsanti 2002) indicates a wide range of colors for minor bodies in the outer Solar System ($0.5 < V - I < 1.8$) while the Sun has $V - I = 0.69$. However, the statistics are still poor since only $\sim 10\%$ (or about 150) of the known KBOs have their color measured. Scaling from the current KBO discovery rate with NOAO 4m telescopes (Millis et al. 2002), we can expect 20-30 new KBOs in each of the GOT and Sgr fields.

4. Instrumentation and Reduction Techniques

With CCD detectors there are three basic modes to obtain an image. Most common is the guided stare-mode, identical to photographing the sky. Alternatively, one may either stop the telescope and let the sky drift across a CCD (drift-scanning mode) or drive the telescope at a rate that is synchronous with the charge transfer rate applied to a CCD (TDI – time delay & integrate mode) as in the SDSS (Pier et al. 2003). In these last two modes, parts of a sky image are formed sequentially in time, which leads to a partial loss of information about the atmospheric noise – a key factor limiting the accuracy of ground-based wide-field astrometry. In the following section we consider only the stare-mode.

The coordinates of astronomical objects in the frame of a detector always contain instrumental effects mainly caused by the imaging optics, known as geometric distortions. In the case of ground-based observations, on top of these distortions one must deal with the effects of atmospheric refraction, which changes the path of incoming light as a function of zenith distance and wavelength. At a microscopic level, atmospheric refraction is highly variable and has very short temporal and spatial coherence intervals. Ordinary CCD devices operating in a static light-integration regime cannot account for such high frequency and spatially unstable effects, other than to expect that longer integration times tend to average them out. Indeed, both theoretical predictions (Lindegren 1980) and empirical relationship, e.g., Zacharias (1996) indicate that the uncertainty in positions due to atmospheric noise is proportional to $t^{-\frac{1}{2}}$, where t is the integration time. However, there is a fine line between the desire to extend the integration time and the danger of image saturation. As a result, one

usually ends up with a less than optimal exposure time (too short) which inevitably includes a substantial non-modellable contribution of atmospheric noise which limits the astrometric accuracy.

The first step in astrometric reductions is to derive distortion-free coordinates. This normally involves some external reference frame although there is a way to self-calibrate the distortion, at the expense of an unknown absolute scale factor (Anderson & King 2003) and with a caveat that the concept has been proven for the space-based HST observations only. Here we will consider the case with reference frames, first in a single CCD chip regime and then with a CCD mosaic.

4.1. Single CCD detector

Astrometry with single CCD chips is very similar to astrometry with a photographic plate. First, the celestial coordinates of reference stars are converted into standard coordinates via the gnomonic (TAN) projection of a sphere onto the plane at a tangent point. Then, the measured Cartesian coordinates of the reference stars are adjusted to their standard coordinates using least-squares as a maximum likelihood estimator. This step involves a plate model which, besides coordinate offset, rotation, and scale factor, should also adequately represent all other significant effects such as tilt and geometric distortions. Finally, the calculated standard coordinates are projected back onto the celestial sphere. In certain applications, and in the case of poor sets of reference stars, it is desirable to pre-correct the measured coordinates for tilt and distortions, if they are constant.

A couple of potential problems may arise in CCD astrometry. First, the field-of-view may be too small and not contain a sufficient number of reference stars. Second, the images of brighter stars, which typically are the best reference stars, may be saturated and unsuitable for precise measurements. In either case, the plate model parameters are not satisfactorily constrained. In other words, the accuracy of the resulting celestial coordinates could be much lower than the precision of the measured Cartesian coordinates. Differential astrometry employing the measured coordinates can yield very high precision. Thus, Pravdo & Shaklan (1996) have achieved a 1 mas precision over a few arc-min field. Similarly, the USNO parallax program with the 1.55 m telescope routinely produces relative astrometric measurements accurate to 3 mas per epoch (Dahn et al. 2002), which then lead to a sub-mas precision in parallaxes over several years of observations. These quoted values though must be qualified by the caveat that extreme care was taken to minimize all potential sources of systematic and random errors.

This classical astrometric reduction scheme certainly has limitations stemming from a limited precision and possible systematic errors in the reference star catalogs. Any position, magnitude, or color dependent error in the reference stars will propagate into the distortion coefficients and target star positions.

4.2. CCD mosaic device

Large CCD mosaic devices for direct imaging are now available for many telescopes of different sizes (Groom 2000), and they indeed dramatically increase the productivity of these facilities. However, we cannot ignore the fact that an array of CCDs is a fragmented detector consisting of separate units, each with its own characteristics. For astrometry, it is extremely inconvenient to have a 'broken-up' focal plane assembly. Therefore, it is not surprising that, for instance, at the NOAO 4m Blanco and Mayall telescopes a common practice is to extend the concept of one-chip astrometric reductions to each individual chip in the mosaic (Davis 1998). The NOAO Mosaic Imagers include eight thinned, back illuminated, 2K×4K SITe CCDs. Thus, each solution, or a set of plate constants in the FITS header, contains information on the optical distortion and the chip location relative to the telescope's optical axis. The plate constants are determined at the beginning of an entire run, during which the telescope zeropoint may change, and hence a repeat off-line solution with USNO-B or UCAC stars safeguards against possible shifts in predicted coordinates, cf. (Millis et al. 2002).

The obvious simplicity and convenience of chip-oriented solutions nonetheless neglect two basic facts: 1) the bulk of geometric distortions produced by the optical system is axicentric and can be quantified by a *single* set of constants for the whole CCD camera; 2) there is only one projection of the celestial sphere onto the focal plane at a single tangent point. These two properties essentially demand unification of the fragmented detector into a single superplate, characterized by a common Cartesian coordinate system, x, y. Such a superplate then allows us to enlarge the number of reference stars by a factor equal to the number of CCD chips and to *reduce* the number of unknown constants by nearly the same factor. A set of the so-called chip constants – the x_i, y_i position of the i-th chip center, a rotation angle, Θ_i, around this center, and a look-up table of higher-frequency distortions emanating from imperfections of the CCD surface (non-planarity, small tilt, and twisted/skewed pixel axes) – then fully describe each chip's metric (Platais et al. 2002).

Perhaps one of the earliest efforts to develop the superplate concept is the work by Kaiser et al. (1999), later implemented by the Terapix[1] data reduction center aimed at complete and

[1]http://terapix.iap.fr

automated reductions of large datasets such as the output from the CFHT 3.6m telescope with the MegaPrime CCD mosaic imager. To better understand the astrometric properties of CCD mosaics, Platais et al. (2002) examined in great detail the NOAO CCD Mosaic Imager by using an astrometric standard field. The summary of this study is given in the following section.

4.2.1. The techniques

The technique of deriving the metric of a CCD mosaic using an astrometric standard is straightforward – the measured pixel coordinates of reference stars, X_p, Y_p, must be adjusted to their tangential coordinates, ξ, η, calculated via the gnomonic projection. Following the concept of a superplate, the pixel coordinates, X_p, Y_p, should be translated into the global Cartesian CCD coordinate system x, y. That can be done indirectly through the reference stars and a least squares adjustment $x, y \Longrightarrow \xi, \eta$, employing an appropriate polynomial plate model (including all distortion terms). Consider that we have derived a set of approximate values for the chip centers and rotation angles cx_i, cy_i, Θ_i and, hence, the global coordinates x, y. Usually, the initial chip centers are estimated from the measured chip separations but rotation angles can be safely assumed to be zero. Apparently, the adjustment $x, y \Longrightarrow \xi, \eta$ with such crude global coordinates will produce very poor residuals, reflecting our first guess for the chip constants. In order to improve them, we should select a fixed set of reference stars and minimize the standard error, σ, of the adjustment $x, y \Longrightarrow \xi, \eta$ while searching through the parameter space cx_i, cy_i, Θ_i at a fixed i. In other words, an adjustment, equivalent to χ^2, is used to find iteratively an i-th triad of the chip constants cx_i, cy_i, Θ_i, one at a time. It is the minimum of the standard error σ, that signals that the chip constants have been found. Normally, the next step is to find the distortion center and refine the geometric distortion terms, using the same adjustment but now adopting the obtained mean chip constants (Platais et al. 2002).

In practice, the chip constants derived in this way are sensitive to the achieved accuracy of geometric distortion determination. Since geometric distortions are stable over the timespan of fixed optical adjustment of a telescope, it is desirable to pre-correct the pixel coordinates X_p, Y_p for geometric distortions, provided the optical center (tangent point) is known or can be found. This allows simplification of the plate model down to linear terms only. The repeated adjustments of the values of the chip constants with a linear model provide more accurate chip constants. The accumulated residuals from these adjustments then allows one to generate a look-up table of the higher-frequency, unmodelled, distortions.

Limited accuracy and low density of reference stars are some of the other factors that

may affect the precision of the chip constants. If this is a serious problem, then self-calibration techniques can provide a solution (Anderson & King 2003). This approach makes use of *all* images in the overlapping area. The advantage of self-calibrating techniques is a higher number of stars and the presence of only one source of random errors, that is the errors from image centering. The disadvantage is a large number of overlapping frames required to achieve high precision and an inability to derive the absolute scale.

The strongest test this technique has faced so far is in calculating proper motions in the open star cluster NGC 188 from a combination of old photographic plate measurements and the CCD mosaic data (Platais et al. 2003), which resulted in a 0.15 mas yr^{-1} accuracy and indicated no apparent systematic errors.

4.2.2. A pilot study around NGC 188

As a by-product of the WIYN Open Cluster Study (WOCS), we have created a relatively deep ($V \leq 21$) astrometric standard in the 0.75 deg^2 area around the open cluster NGC 188 (Platais et al. 2003). It is based upon 30 old photographic plates from assorted large-aperture telescopes, in combination with more than a 100 CCD mosaic frames obtained at the KPNO 4m telescope with the NOAO CCD Mosaic Imager. The plate measurements and the global CCD coordinates x, y of each frame, as described in Sect 4.2.1, were mapped into the specifically constructed (Platais et al. 2002) Lick intermediate catalog of positions and proper motions around NGC 188. The Lick intermediate catalog is similar to UCAC in terms of limiting magnitude at $V \sim 17$, positional precision ($\sim$ 60 mas or better), and proper motion accuracy (2-7 mas yr^{-1}).

The WOCS astrometric standard for optimally exposed isolated stars yields a 2 mas precision in positions. At the time it was believed that the positions are within ∼5-10 mas on the system of ICRS (Platais et al. 2003). However, a detailed comparison with the preliminary UCAC data in that area of the sky shows much larger systematic positional differences. There is a clear spatial trend in the differences 'UCAC-WOCS' indicating a scale problem (Fig. 2). In other words, a $\sim$ 6.5 mas per arcmin correction in both axes would bring the two systems of coordinates to a nearly perfect match. The observed systematic differences are unexpected since in both cases the astrometric reductions were done using the Tycho-2 catalog, albeit utilizing different sub-samples and, in the case of WOCS standard, indirectly via the Lick intermediate catalog. It should be noted that the Lick intermediate catalog, used as a reference frame in Platais et al. (2003), contains magnitude-dependent systematic errors. This is demonstrated by direct coordinate differences 'Lick-WOCS' (Fig. 3,4). The common Tycho-2 stars, indicated by the filled squares, show a considerable offset (up to

$\sim$ 90 mas) between the two catalogs. Additional tests, involving the UCAC and 2MASS positions, show that it is the Lick intermediate catalog responsible for this kind of systematic error. Nevertheless, such magnitude-dependent systematic errors alone should not introduce a spatial trend in the coordinates of the WOCS astrometric standard. At this point we cannot identify unambiguously the source of the spatial trend.

A large number of CCD Mosaic frames around NGC 188 allows us to obtain some statistics on the residual scatter as a function of FWHM and exposure time. The coordinates of all frames were subtracted from the final catalog (Platais et al. 2003) and, after some trimming, the mean dispersion, $\sigma_{\rm pos}$, was calculated for each exposure. As indicated by Fig. 5, there is a strong correlation between the FWHM of images and $\sigma_{\rm pos}$. The dependence on exposure time is almost nonexistent at FWHM$<$ 6 pixels. Apparently, a 30 s exposure is already sufficient to reach the floor of dispersion distribution at $\sim$ 20 mas, at least for the zenith distances and seeing conditions prevailing at the time of these observations.

This case underscores the uncertainty in linking a catalog to the ICRS, at least over a small area ($\leq$ 1 deg^2). It should also be noted that, as a circumpolar object, NGC 188 is always at large zenith distance ($z > 53^\circ$ from Kitt Peak) and over 60% of all frames were taken with short exposures ($\leq$ 30 s), thus were exposed to deleterious atmospheric effects on astrometry. With longer exposures, a near zenith pointing, and in sub-arc-sec seeing high positional precision can be achieved with a substantially smaller number of CCD mosaic frames – as planned for the DAS observations.

4.2.3. Astrometry with the Subaru Suprime-Cam imager

In the context of LSST it is instructive to consider a telescope with a similar aperture to LSST. The Subaru 8.2m telescope is the only one in its class having a mosaic CCD imager with large FOV ($34' \times 27'$). We used the SMOKA Science archive[2] and extracted ten short exposure Suprime-Cam CCD mosaic (Miyazaki et al. 2002) frames of the ESP field 1 in the Sloan i'-filter taken in May 7, 2002 (Monet & Platais 2004). The corresponding sub-frame identificators span SUPA00106300-SUPA00106399. On these frames, more than 400 UCAC stars can be identified. Many of them are overexposed but surprisingly without a substantial degradation in the positional precision. Following the notation in Platais et al. (2002), the original pixel coordinates, X_p and Y_p (D. Monet, private communication) were used in deriving preliminary chip constants and the optical field angle distortion (OFAD) parameters. The geometric center for the entire CCD frame was adopted at x_c=5300 and

[2]http://smoka.nao.ac.jp

y_c=4100 pixels. The derived chip constants are given in Table 2, which contains the chip number, the chip constants, dx and dy, in pixels and the rotation angle, Θ, in radians. The corresponding CCD layout is given in Fig. 6. The standard error estimates, ϵ_{dx}, ϵ_{dy}, and ϵ_Θ, are for a single determination of the chip constants. It should be emphasized that these constants are valid only for the epoch 2002.3, and extrapolating to other epochs requires additional studies on the stability of the chip constants.

The cubic distortion term in the i' bandpass is $(-4.767 \pm 0.012) \times 10^{-16}$ rad pixel^{-3} in right ascension and $(-4.674 \pm 0.017) \times 10^{-16}$ rad pixel^{-3} in declination. The fifth order term along the same axes is $(+2.11 \pm 0.03) \times 10^{-24}$ rad pixel^{-5} and $(+1.89 \pm 0.03) \times 10^{-24}$ rad pixel^{-5}. The reason for providing separate distortion solutions in each axis is to show their consistency, which may vary from one telescope to another indicating subtle deviations from a perfect reference frame and/or optical system itself, and possible pixel scale differences along the x and y axes. For practical applications, distortion solutions should be averaged.

We note that the 5th order term indicates the presence of a barrel-type distortion while the cubic distortion is the pincushion type. A similar conclusion can be drawn from the optical distortion parameters derived in Miyazaki et al. (2002), although they used a different field-distortion model. The global (whole-frame) solutions using over 400 UCAC reference stars routinely yielded a standard deviation of 40 mas or better. The contribution of uncertainties in the reference frame is estimated to be around 30 mas, leaving $\sim$ 20 mas attributable mainly to unmodelled systematic errors in the positions. The Suprime-Cam camera appears to have excellent astrometric properties.

The main purpose of these astrometric solutions was to explore atmospheric effects in 10 s and 30 s exposures. All ten sets of equatorial coordinates were combined to derive a catalog in the direction of ESP field 1 (RA=$18^{\rm h}26^{\rm m}$, Dec=$+21^\circ42'.3$, J2000). The coordinate differences between the catalog and a selected CCD mosaic frame should be representative of atmospheric noise. Apparently, these differences (or residuals) will also include the modelling error, mainly originating from the least-squares adjustment to obtain the equatorial coordinates. The contribution of modelling error, however, is kept constant by using frames with identical telescope pointing, the same plate model, and essentially the same reference stars in all frames.

A distinct advantage of this approach is the possibility to probe atmospheric noise over the scales substantially larger than the chip size. That is clearly demonstrated by Figs. 7,8 in which the vectorial pattern is consistent between adjacent chips. On average the residual vectors from a 10 s exposure (Fig. 7) are almost twice as long as from a 30 s exposure (Fig. 8). It is conspicuous that these vectors appear to have a prevalent North-South direction, albeit atmospheric noise should be acting randomly. This unusal phenomenon clearly requires

further studies. It should be noted that the Suprime-Cam frames considered in this study have not been obtained under optimal conditions. For instance, the guiding was off and that resulted in somewhat asymmetric images. Nevertheless, on the 30 s exposure frames it is possible to isolate narrow but long, up to $25'$, stretches of the sky showing residual scatter at the level of only 3 mas. On the 10 s frames, the extension of such low-residual areas is much shorter – on the order of $5'$ only. This appears to be indicative of the area on the sky where high-precision differential astrometry, reaching the intrinsic error floor, is feasible with short exposures.

4.3. Limitations in CCD mosaic astrometry

The major source of uncertainties in this technique is the limited positional accuracy of a reference catalog and/or insufficient number of reference stars. The typical FOV of existing large telescopes equipped with a CCD mosaic is about 0.4 deg^2. The CFHT MegaPrime camera covers nearly a full square degree which probably is an upper limit for this type of telescope unless a new type of wide-field field corrector can be manufactured (Epps & DiVittorio 2003; Komiyama et al. 2004). Another critical number is the typical centering precision of 0.02-0.05 pixels for optimally exposed stellar images on the CCD mosaic (Platais et al. 2002). That translates into a 5-15 mas precision for the average pixel size of $\sim 0\farcs2 - 0\farcs3$. How many reference stars of comparable positional accuracy can we find in a typical square degree on the sky? Near the Galactic plane the density of UCAC stars, $n_{\rm U}$, is indicated in Table 1. In the case of the NOAO 4m telescopes and their CCD mosaics that amounts to ∼500-1300 stars over the FOV. If only that many stars are used to derive geometric distortions and chip locations, all at once, the chances are that the solution may not provide the desired accuracy. Therefore, additional constraints available from the areas of overlapping frames are vital to reach a 5-10 mas precision across a larger FOV. We stress here that the most important aspect of wide-angle astrometry is the astrometric flat-fielding, so that the transformation of any two overlapping fields or frames is purely conformal, i.e., limited to offset, rotation, and scale only. The mapping accuracy into the ICRS is then entirely dependent upon the degree to which a concrete reference frame represents the ICRS.

There are two significant factors that potentially can limit the astrometric accuracy with CCD mosaics:

1. Atmospheric turbulence puts a fundamental limit on the temporal and spatial precision of astrometry in accordance with the predictions from Lindegren (1980) and the positional variance analysis from CCD observations (Zacharias 1996). Thus, over the

angular extension of the CCD Mosaic's chip at the KPNO 4m telescope (18′) the standard deviation of the atmospheric noise contribution in a 10 s exposure is $\sim$ 30 mas (Platais et al. 2002). The effect of atmospheric noise is illustrated in Fig. 9, which shows the coordinate differences from two consecutive exposures. It can be reduced only by averaging multiple short exposures or by extending the exposure time.

2. CCD mosaic devices require frequent monitoring of their metrics. For instance, thermal cycling may trigger a nonelastic change in the geometry of the CCD chips as it did in the KPNO CCD Mosaic Imager (Platais et al. 2002).

4.4. DAS observations & reduction techniques

In previous sections we have shown that a deep high-precision astrometric standard is feasible and indeed vital in calibrating the FPA. The NOAO 4m telescopes and their CCD mosaic imagers are well suited to reach the desired magnitude range ($10 < V < 25$) and spatial coverage (10 deg^2). The bright end of the magnitude range, $10 < V < 16$, includes the UCAC stars – the best existing dense reference frame. In order to cover the DAS magnitude range and reach stars at $V = 25$ with S/N=7 or better, a set of 10 s, 120 s and 900 s exposures is required at each telescope pointing.

To achieve the science goals and account for differential color refraction (DCR), imaging will be done in Johnson-Cousins VI filters. For astrometry, it is preferable to observe at longer wavelengths where atmospheric refraction is smaller, hence $\sim$ 70% of our observations will be obtained in the I bandpass. To reach the *accuracy* of 5-15 mas (see Sect. 4.3) across the entire DAS field and iron out all systematic position-, color-, and magnitude-dependent errors, multiple passes are required in the I bandpass, each at 0′, 6′, 12′, and 18′ dithers. This is an absolute minimum of passes needed to apply the block-adjustment and self-calibration techniques which are crucial to the success of the DAS project. Two additional passes are necessary to obtain seamless V photometry, which enhances the astrometric precision in addition to providing star counts. Thus, a total of six complete passes per DAS field are required. In order to obtain absolute proper motions of all stars relative to faint QSOs and compact background galaxies, the same sequences should be repeated after 3-4 years.

The large number of frames – on the order of 700 per DAS field at one epoch – compel usage of unsupervised reduction techniques. A variant of DOPHOT (Schechter, Mateo & Saha 1993) with variable point-spread function, developed at NOAO, is our choice in obtaining the pixel coordinates for all objects in the DAS fields. Custom-built software to analyze astrometric CCD data (L. Winter, private communication) would be used at the

US Naval Observatory to process the same frames. Thus, similar to Hipparcos, a two-team effort will ensure quality control and provide the means to identify any weaknesses in the reductions.

Two high-precision local astrometric standards – NGC 188 in the northern hemisphere (Platais et al. 2002) and ω Cen in the south (van Leeuwen et al. 2000; Platais et al. 2005) will be used to derive the chip constants and refine the distortion coefficients. These parameters and improved look-up tables of higher-frequency distortions (mainly due to non-planarity and small tilt of the CCD chips and wave-front errors in the optical elements) will then fully describe each chip's metric. Distortion free Cartesian coordinates x, y then can be bootstrapped using a direct plane-to-plane transformation (Makovoz 2004) which allows us to obtain a 'superplate' of the desired size, e.g., 10 deg^2. The final step is to convert the superplate's Cartesian coordinates into the UCAC (Zacharias et al. 2004) via a robust linear plate model, thus minimizing possible local spatial errors in the ICRS representation by UCAC. The expected accuracy of the final coordinates should be in the range of 5-10 mas, if a star is observed at least six times with optimal exposure. This is 3 to 10 times better than any existing large positional catalog can offer. Up to 50% of an overlap between the frames should further strenghten the reliability of superplate coordinates by applying the block-adjustment (Zacharias 1992) and the so-called residual technique successfully tested on the HST WFPC2 camera (Anderson & King 2003).

4.5. Linking to ICRF

As described in Sect. 2 and shown on the actual application in Sect. 4.2.2 the uncertainties in linking a catalog to the ICRS are far larger than the precision level would indicate. There is a way to substantially reduce these uncertainties if we are able to translate the superplate directly into the International Celestial Reference Frame (ICRF). The positional accuracy of individual extragalactic radio sources defining the ICRF is $\sim$ 0.25 mas (Fey et al. 2004). Unfortunately, a very low sky density of these sources ($<$ 1000 over the entire sky) currently prevents a direct link to the ICRF. We propose a local densification of the ICRF in the direction of the DAS fields. That can be done, for example, by selecting strong sources from the NRAO VLA Sky Survey (NVSS) at 1.4 GHz (Condon et al. 1998). Thus, in the GOT field (see Sect. 3.3), the NVSS contains 26 strong sources ($S \gtrsim 60$ mJy), which are expected to be predominantly classical radio galaxies and QSOs. One source in this field, J0603+2159, has already made the list of VLBA Calibrator Survey (Fomalont et al. 2003). More detailed VLBI observations in the standard S and X bands should provide high-accuracy (1-5 mas) positions of the NVSS strong sources. The low spatial resolution

of the NVSS survey at $\Theta = 45''$ FWHM does not yield information on the source structure, hence the real number of useful point sources is unknown. The optical counterparts of point sources should provide the reference fiducials to the ICRF. If the number of these fiducials is approaching, say, ten, a direct solution into the ICRF is quite feasible. In the case of a lower number of reference fiducials, we are limited to zeropoint differences only. In either case the external accuracy will be constrained much better than just by using the faint end of the UCAC.

It should be mentioned that a high-accuracy link to QSOs requires a high-precision correction for differential color refraction (DCR). The main source of uncertainty in DCR is a marked difference between the spectral energy distributions (SED) for stars and QSOs. To derive SED of QSOs, low-resolution spectrophotometry of their optical counterparts is highly desirable.

5. Conclusions and recommendations

The main goal of this paper is to provide a rationale for Deep Astrometric Standards. We have shown that DAS are vital for the next generation of imaging telescopes designed to map out the 3-dimensional mass distribution in the Universe. The underlying very subtle effect of galaxy weak lensing requires that the Focal Plane Array be astrometrically extremely well calibrated. Establishing the DAS is the only reasonably way at this time to perform such calibrations at the level of a 5-10 mas precision.

Although the DAS concept primarily serves the needs of astrometric calibrations for large telescopes, full consideration is given to other benefits that such fields can provide to astronomy. The selection of the first DAS fields is well-optimized to the needs of studies of Galactic structure and kinematics, especially for the thick and thin Galactic disks.

Since the minimum amount of observing time to create a single DAS field at one epoch with existing CCD mosaic imagers is about 100 hrs, the DAS initiative may require an international collaboration among observatories that have at least a 3m aperture telescope and an imager with detector collecting area covering $\gtrsim 0.25$ deg^2. If there is enough interest in the community, the same fields can also serve as faint photometric standards, but that would require additional imaging in the desired bandpasses. To acquire a proper-motion component of the DAS, the imaging should commence as soon as possible and then be repeated 3-4 years later. The targeted accuracies are 5-10 mas in positions and 2 mas yr^{-1} in proper motions down to V=25. The DAS will be the only faint and accurate standards in the pre-GAIA period and may serve well over 1-2 decades.

The authors thank David Monet for supplying object coordinates for the selected archival frames taken with the Subaru Suprime-Cam imager. One of the authors, I.P., thanks Megan Sosey for the excellent observations she obtained for us with the KPNO 4m telescope and Aaron Romanowsky for observing the Sgr field at the CTIO 4m telescope. We thank the referee for thoughtful comments and questions. This study is based in part on data collected at the Subaru telescope and obtained from the SMOKA science archive at the Astronomical Data Analysis Center, which is operated by the National Astronomical Observatory of Japan. This work has been supported in part by National Science Foundation grant AST 04-06689 to Johns Hopkins University (I. P.) and by NASA grant HST-AR-09958.01-A (RFGW and I. P.). awarded by the Space Telescope Science Institute, which is operated by the Association of Universities for Research in Astronomy, Inc., under NASA contract NAS5-26555.

REFERENCES

Abadi, M. G., Navarro, J. F., Steinmetz, M., & Eke, V. R. 2003, ApJ, 597, 21

Anderson, J., & King, I. R. 2003, PASP, 115, 113

Beers, T. C., Prieto, C. A., Wilhelm, R., Yanny, B., & Newberg, H. 2004, PASA, 21, 207

Bellazzini, M., Ibata, R., Monaco, L., Martin, N., Irwin, M. J., & Lewis, G. F. 2004, MNRAS, 354, 1263

Chiu, L.-T. G. 1980, ApJS, 44, 31

Claver, C. F., et al. 2004, Proc. SPIE, 5489, 705

Condon, J. J., Cotton, W. D., Greisen, E. W., Yin, Q. F., Perley, R. A., Taylor, G. B., & Broderick, J. J. 1998, AJ, 115, 1693

Cutri, R. M., et al. 2003, Explanatory Supplement to the 2MASS All Sky Data Release (Pasadena: IPAC)

Dahn, C. C., et al. 2002, AJ, 124, 1170

Davis, L. E. 1998, in Astronomical Data Analysis Software and Systems VII, ASP Conf Ser. 145, eds. R. Albrecht, R. N. Hook & H. A. Bushouse, (San Francisco: ASP), 184

Dinescu, D. I., et al. 2002, ApJ, 575, L67

Epps, H. W., & DiVittorio, M. 2003, Proc. SPIE, 4842, 355

ESA 1997, The Hipparcos and Tycho Catalogues (ESA SP-1200) (Noordwijk: ESA)

Famaey, B., Jorissen, A., Luri, X., Mayor, M., Udry, S., Dejonghe, H., & Turon, C. 2005, A&A, 430, 165

Le Fèvre, et al. 2004, A&A, 417, 839

Fey, A. L., et al. 2004, AJ, 127, 3587

Fomalont, E. B., Petrov, L., MacMillan, D. S., Gordon, D., & Ma, C. 2003, AJ, 126, 2562

Gilmore, G. 1981, MNRAS, 195, 183

Girard, T. M., Dinescu, D. I., van Altena, W. F., Platais, I., Monet, D. G., & López, C. E. 2004, AJ, 127, 3060

Gould, A. 2003, ApJ, 583, 765

Groom, D. E. 2000, Proc. SPIE, 4008, 634

Hanson, R. B., Klemola, A. R., Jones, B. F., & Monet, D. G. 2004, AJ, 128, 1430

Hainaut, O. R., & Delsanti, A. C. 2002, A&A, 389, 641

Helmi, A., Navarro, J. F., Nordström, B., Holmberg, J., Abadi, M. G., & Steinmetz, M. 2005, preprint astro-ph/0505401

Hodapp, K. W., et al. 2004, Astron. Nachr., 325, 636

Høg, E., et al. 2000, A&A, 355, L27

Ibata, R. A., Irwin, M. J., Lewis, G. F., Ferguson, A. M. N., & Tanvir, N. 2003, MNRAS, 340, L21

Ivezić, Z., et al. 2004, in Satellites and Tidal Streams, ASP Conf. Ser., vol. 327, eds. F. Prada, D. Martinez Delgado, & T. J. Mahoney (ASP, San Francisco), 104

Jannuzi, B. T., Dey, A., Brown, M. J. I., & Tiede, G. P. 2004, BAAS, 36, 745

Johnston, K. J., et al. 2004, BAAS, 36, 1342

Kaiser, N. 2004, Proc. SPIE, 5489, 11

Kaiser, N., Wilson, G., Luppino, G,. & Dahle, H. 1999, preprint astro-ph/9907229

Komiyama, Y,. Miyazaki, S., Nakaya, H., Furusawa, H., & Takeshi, K. 2004, Proc. SPIE, 5492, 525

Kormendy, J., & Kennicutt, R. C. 2004, ARA&A, 42, 603

Kuijken, K., & Gilmore, G. 1989, MNRAS, 239, 571

Lindegren, L. 1980, A&A, 89, 41

Ma, C., et al. 1998, AJ, 116, 516

Majewski, S. R. 1992, ApJS, 78, 87

Majewski, S. R., Munn, J. A., & Hawley, S. L. 1996, ApJ, 459, L73

Majewski, S. R., Skrutskie, M. F., Weinberg, M. D., & Ostheimer, J. C. 2003, ApJ, 599, 1082

Makovoz, D. 2004, PASP, 116, 971

Marr, J. C. 2003, Proc. SPIE, 4852, 1

Martin, N. F., Ibata, R. A., Bellazzini, M., Irwin, M. J., Lewis, G. F., & Dehnen, W. 2004a, MNRAS, 348, 12

Martin, N. F., Ibata, R. A., Conn, B. C., Lewis, G. F., Bellazzini, M., Irwin, M. J., & McConnachie, A. W. 2004b, MNRAS, 355, L33

Méndez, R. A., Platais, I., Girard, T. M., Kozhurina-Platais, V., & van Altena, W. F. 2000, AJ, 119, 813

Mermilliod, J.-C. 1998, WEBDA Open Cluster Database, http://obswww.unige.ch/webda/

Millis, R. L., Buie, M. W., Wasserman, L. H., Elliot, J. L., Kern, S. D., & Wagner, R. M. 2002, AJ, 123, 2083

Miyazaki, S., et al. 2002, PASJ, 54, 833

Monet, D. G., et al. 2003, AJ, 125, 984

Monet, D., & Platais, I. 2004, BAAS, 36, 1531

Momany, Y., Zaggia, S. R., Bonifacio, P., Piotto, G., De Angeli, F., Bedin, L. R., & Carraro, G. 2004, A&A, 421, L29

Newberg, H. J., Yanny, B., et al. 2002, ApJ, 569, 245

Perryman, M. A. C. 2002, GAIA: a European Space Project, O. Bienaymé & C. Turon, (ESA: EDP Sciences), EAS Publ. Ser 2, 3

Pier, J. R., Munn, J. A., Hindsley, R. B., Hennessy, G. S., Kent, S. M., Lupton, R. H., & Ivezić, Z. 2003, AJ, 125, 1559

Platais, I., et al. 2002, AJ, 124, 601

Platais, I., Kozhurina-Platais, V., Mathieu, R. D., Girard, T. M., & van Altena, W. F. 2003 AJ, 126, 2922

Platais I., et al. 2005, in preparation

Pravdo, S. H., & Shaklan, S. B. 1996, ApJ, 465, 264

Reid, I. N., Yan, L., Majewski, S., Thompson, I., & Smail, I. 1996, AJ, 112, 1472

Robin, A. C., Crézé, M., & Mohan, V. 1992a, A&A, 265, 32

Robin, A. C., Crézé, M., & Mohan, V. 1992b, ApJ, 400, L25

Robin, A. C., Reylé, C., Derrière, S., & Picaud, S. 2003, A&A, 409, 523

Salim, S., & Gould, A. 2002, ApJ, 575, L83

Schechter, P. L., Mateo, M., & Saha, A. 1993, PASP, 105, 1342

Schlegel, D. J., Finkbeiner, D. P., & Davis, M. 1998, ApJ, 500, 525

Siegel, M. H., Majewski, S. R., Reid, I. N., & Thompson, I. B. 2002, ApJ, 578, 151

Tyson, J. A. 2002, Proc. SPIE, 4836, 10

van Leeuwen, F., Le Poole, R. S., Reijns, R. A., Freeman, K. C., & de Zeeuw, P. T. 2000, A&A, 360, 472

van Waerbeke, L., et al. 2000, A&A, 358, 30

Veillet, C., et al. 2001
http://www.cfht.hawaii.edu/Science/CFHTLS-OLD/MSWG/report2.3.ps

Wittman, D., et al. 2002, Proc. SPIE, 4836, 73

Wyse, R. F. G., & Gilmore, G. 1986, AJ, 91, 855

Wyse, R. F. G. 1999, in The Formation of Galactic Bulges, eds. C. M. Carollo, H. C. Ferguson, & R. F. G. Wyse (New York: Cambridge U. Press), 195

Yanny, B., Newberg, H. J., et al. 2003, ApJ, 588, 824

Zacharias, N. 1992, A&A, 264, 296

Zacharias, N. 1996, PASP, 108, 1135

Zacharias, N., et al. 2000, AJ, 120, 2131

Zacharias, N., Urban, S. E., Zacharias, M. I., Wycoff, G. L., Hall, D. M., Monet, D. G., & Rafferty, T. J. 2004, AJ, 127, 3043

Zacharias, N. 2004a, Astron. Nachr., 325, 631

Zacharias, N., Monet, D. G., Levine, S. E., Urban, S. E., Gaume, R., & Wycoff, G. L. 2004b, BAAS, 36, 1418

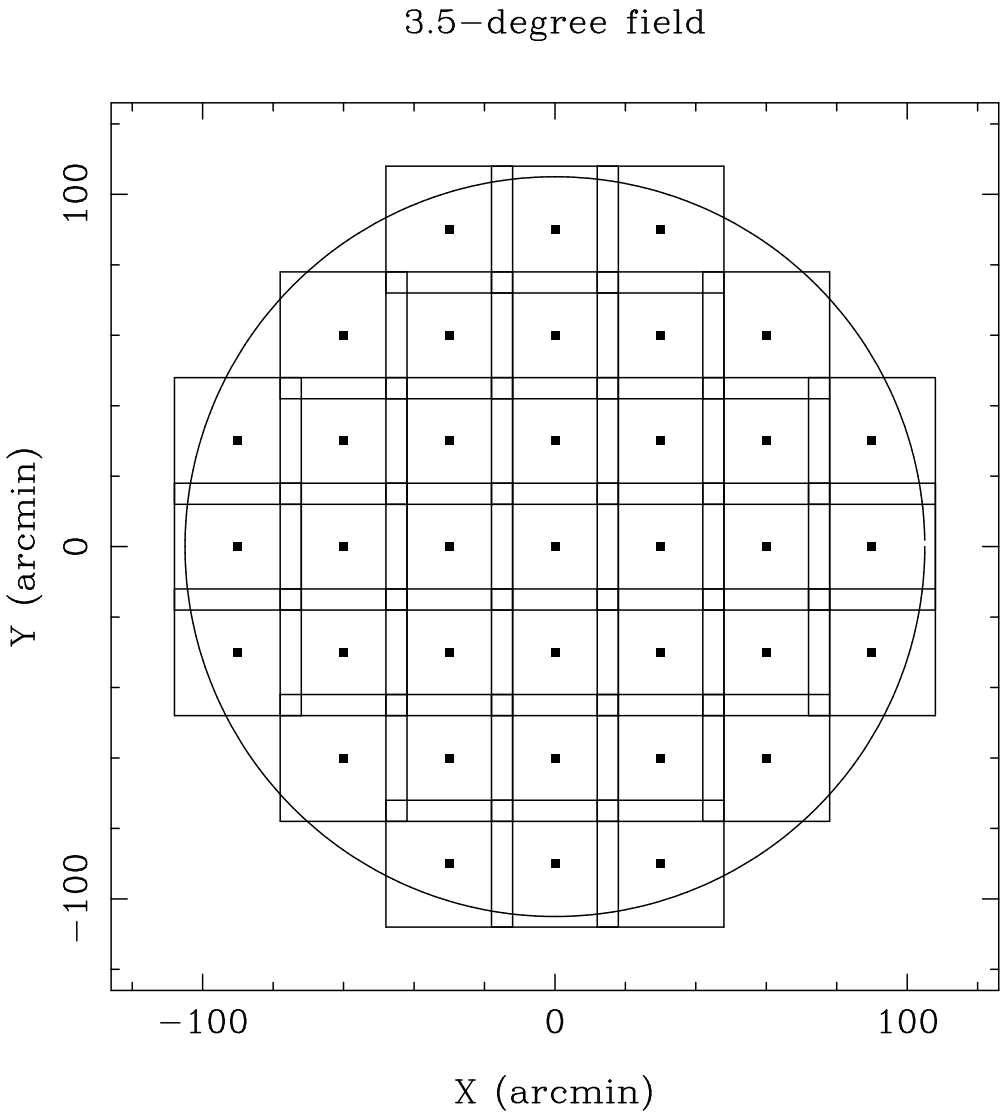

Fig. 1.— Proposed pointing layout in a DAS field with the NOAO 4m telescopes and CCD Mosaic imager. In total, 37 partially overlapping ($\Delta = 6'$) pointings are necessary to fill in a $3.^{\circ}5$-diameter field. The missing parts of the field are filled in by other sets of pointings at large dithers.

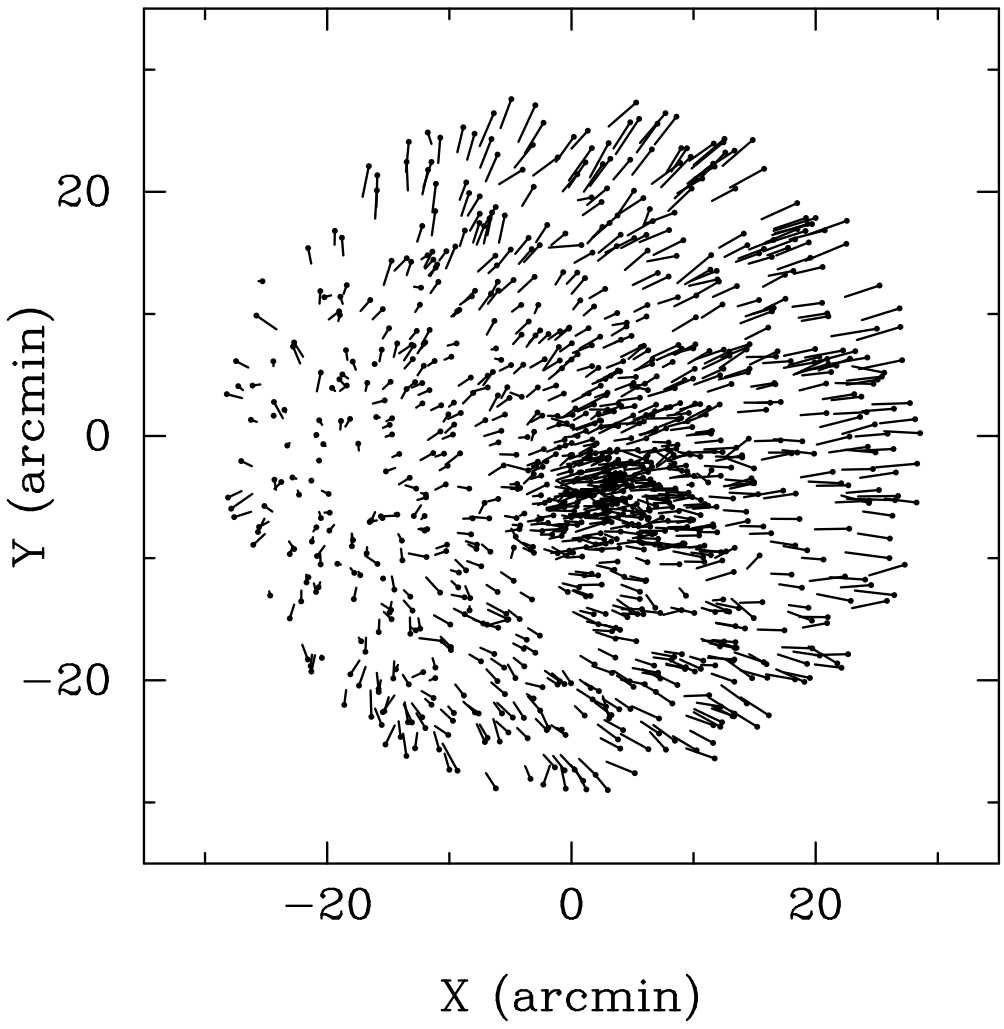

Fig. 2.— Vectorial differences, UCAC–WOCS, around the open cluster NGC 188. The XY axes represent the gnomonic projection of equatorial coordinates with a tangent point at RA=$0^{\rm h}44^{\rm m}20^{\rm s}$ Dec=+85°18′.9 (J200). The largest vector is about 300 mas long.

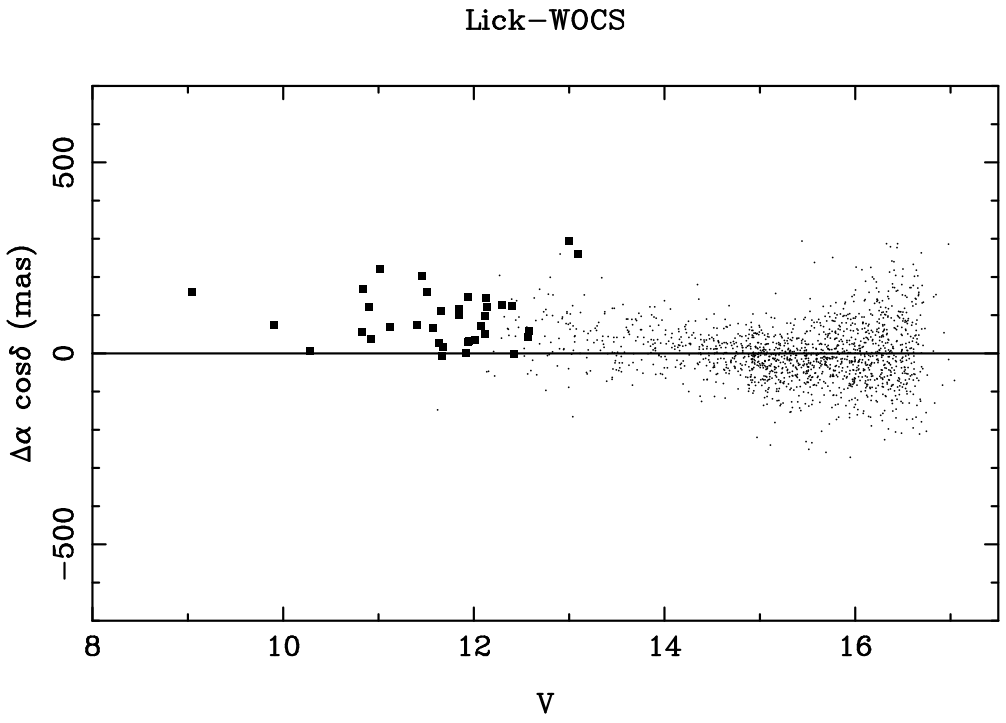

Fig. 3.— Right ascension differences, Lick–WOCS, around the open cluster NGC 188 (Platais et al. 2003). The filled squares indicate the common Tycho-2 stars. In part, the mean offset of these Tycho-2 stars is a measure of the deviation from the ICRS.

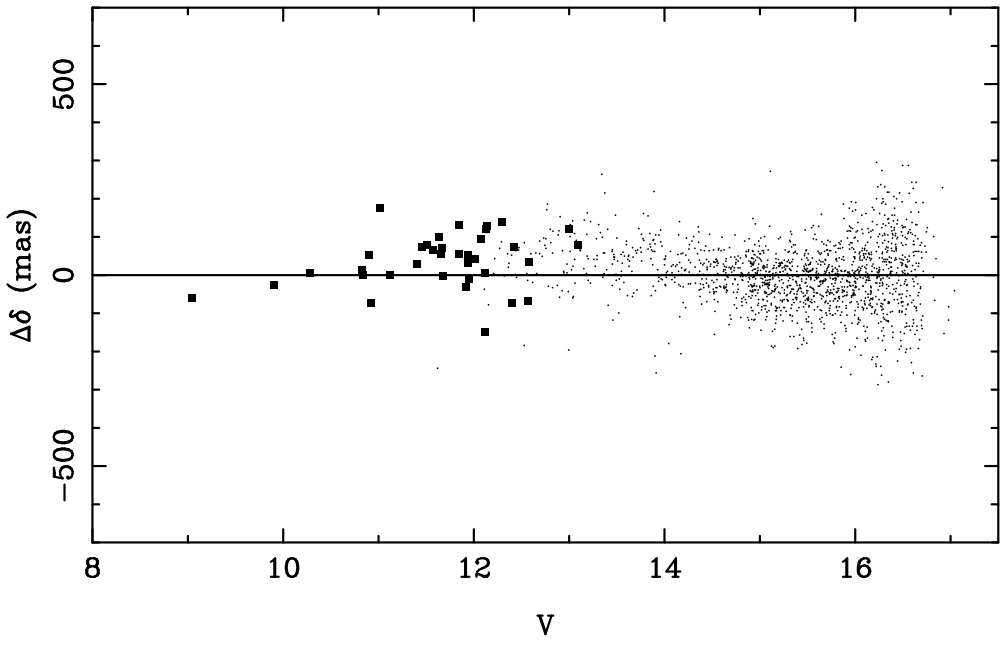

Fig. 4.— Declination differences, Lick–WOCS, around the open cluster NGC 188 (Platais et al. 2003). The filled squares indicate the common Tycho-2 stars.

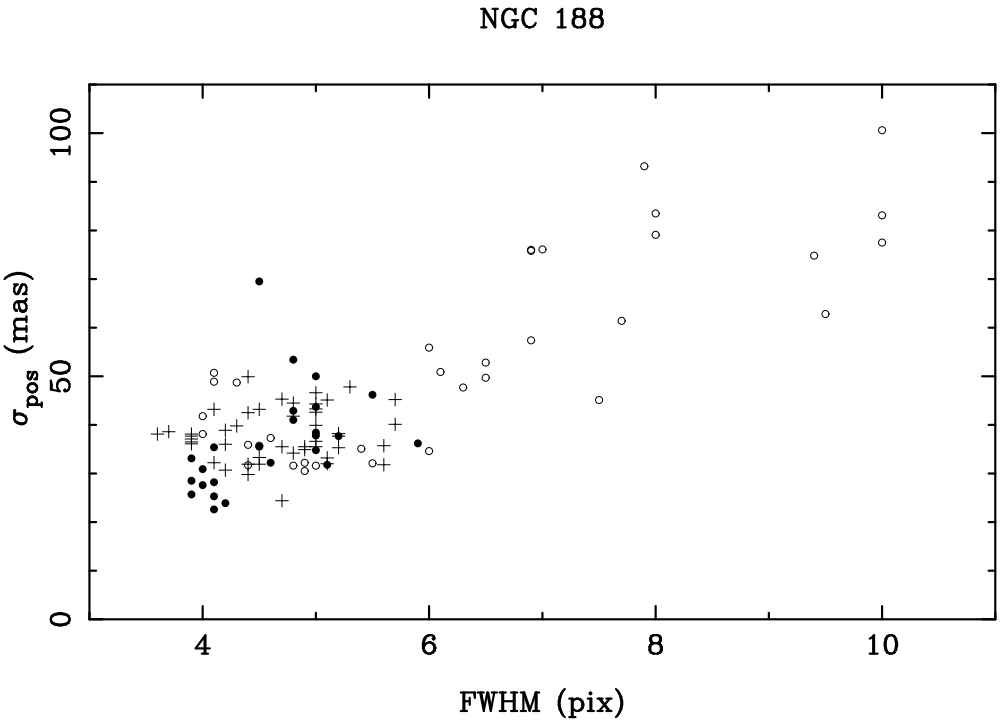

Fig. 5.— Distribution of mean positional dispersions, $\sigma_{\rm pos}$, as a function of FWHM and exposure time. The data around NGC 188 are from the NOAO CCD Mosaic Imager at the Kitt Peak 4m telescope (1 pixel= 0.″26). The open circles denote 10-15 s exposures; bold dots – 30 s; crosses – 120-180 s. In this high zenith distance field ($z > 53^\circ$) the dependence on exposure time is minimal.

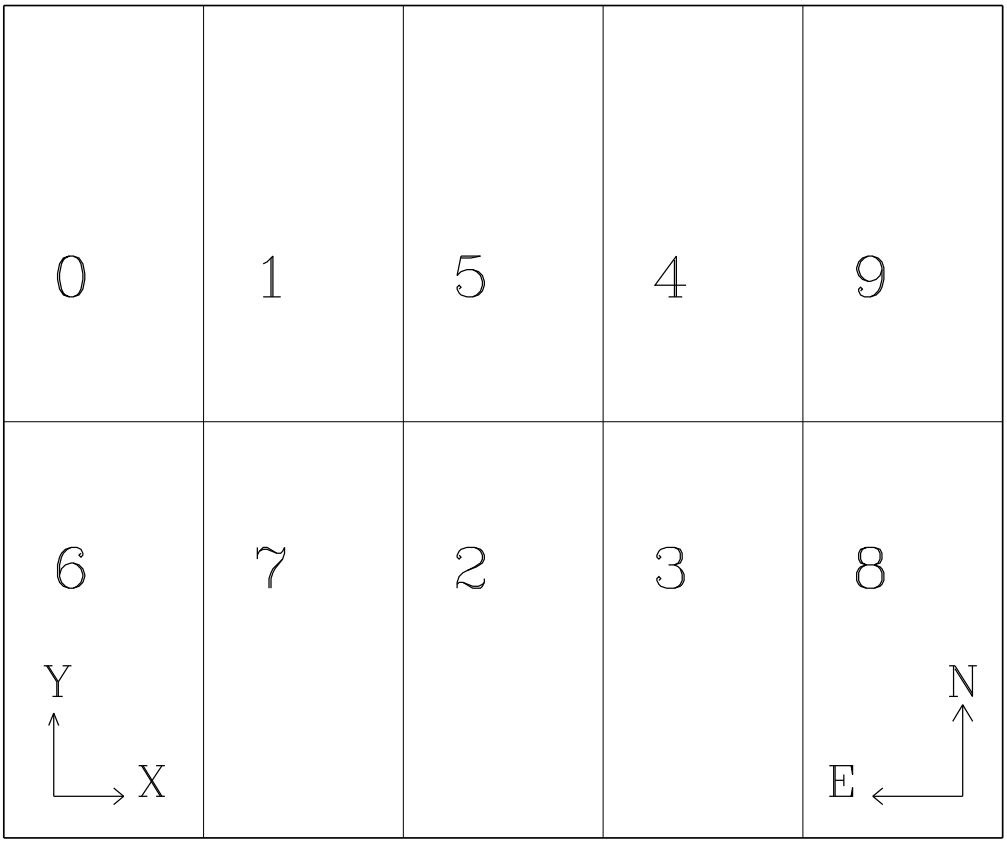

Fig. 6.— Layout of the Subaru Suprime-Cam CCD mosaic imaging plane, showing the adopted chip numbers, the original pixel coordinate axes and the N-E direction.

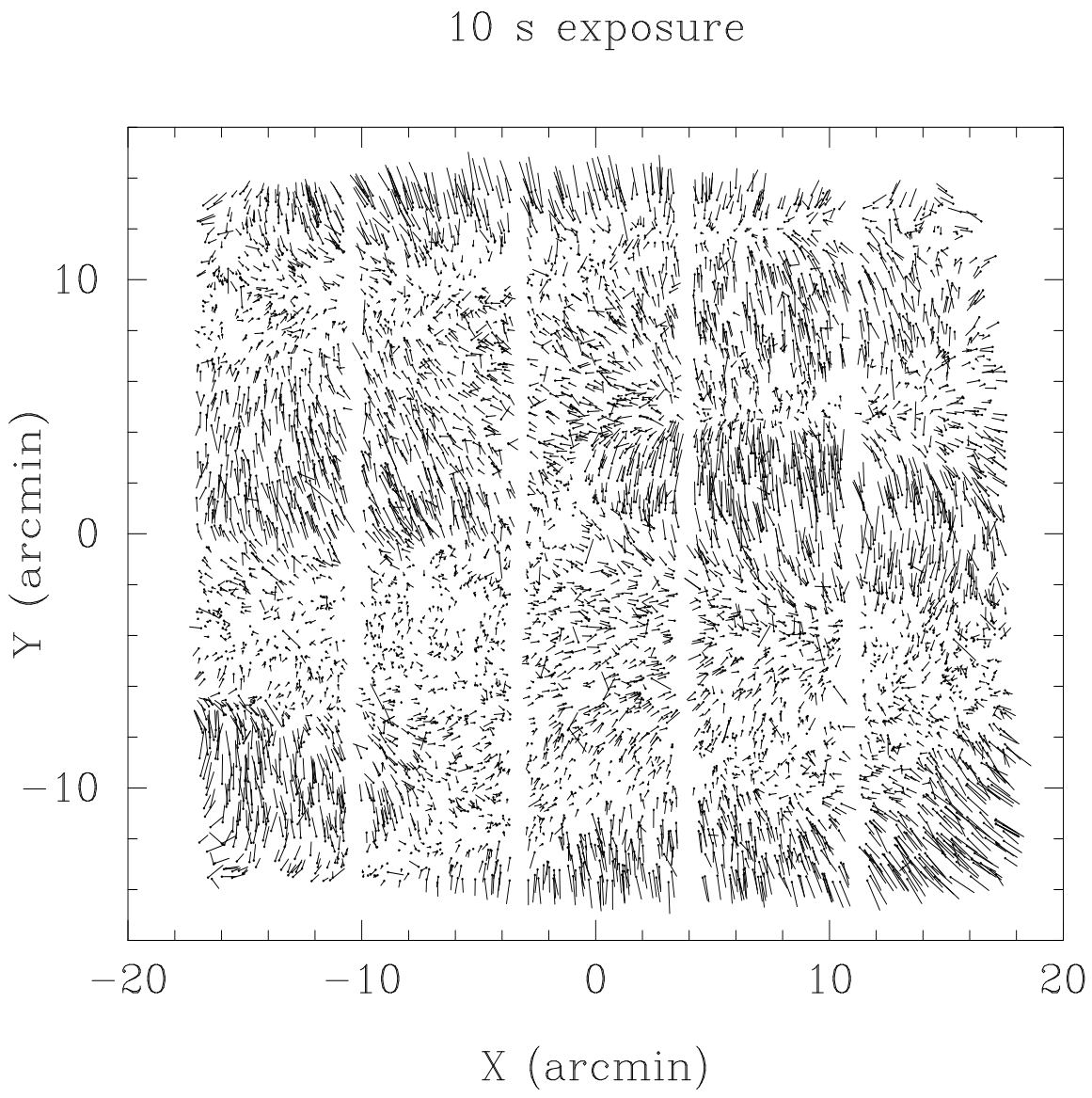

Fig. 7.— Vectorial coordinate differences, catalog–CCD frame, for the image with the Subaru Suprime-Cam. The XY axes represent the gnomonic projection of equatorial coordinates. The selected 10 s exposure shows a correlated pattern of residuals, mostly due to atmospheric noise. The longest vector represents 50 mas.

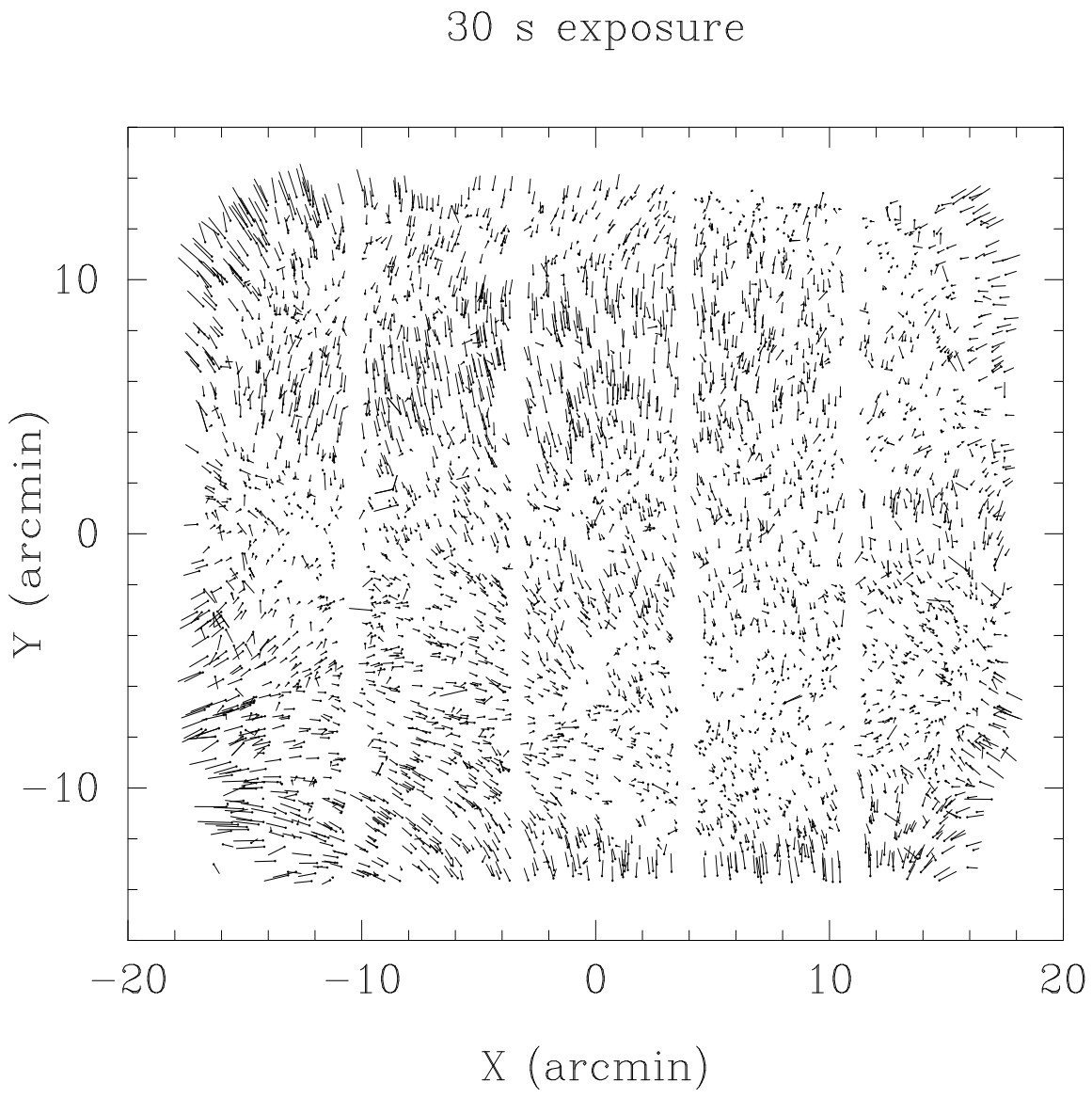

Fig. 8.— Vectorial coordinate differences, catalog–CCD frame, for the image with the Subaru Suprime-Cam. The XY axes represent the gnomonic projection of equatorial coordinates. The distribution of vectors is much smoother than in Fig. 7, although some unmodelled field distortions may be seen at the field edges. The same scale as in Fig. 7.

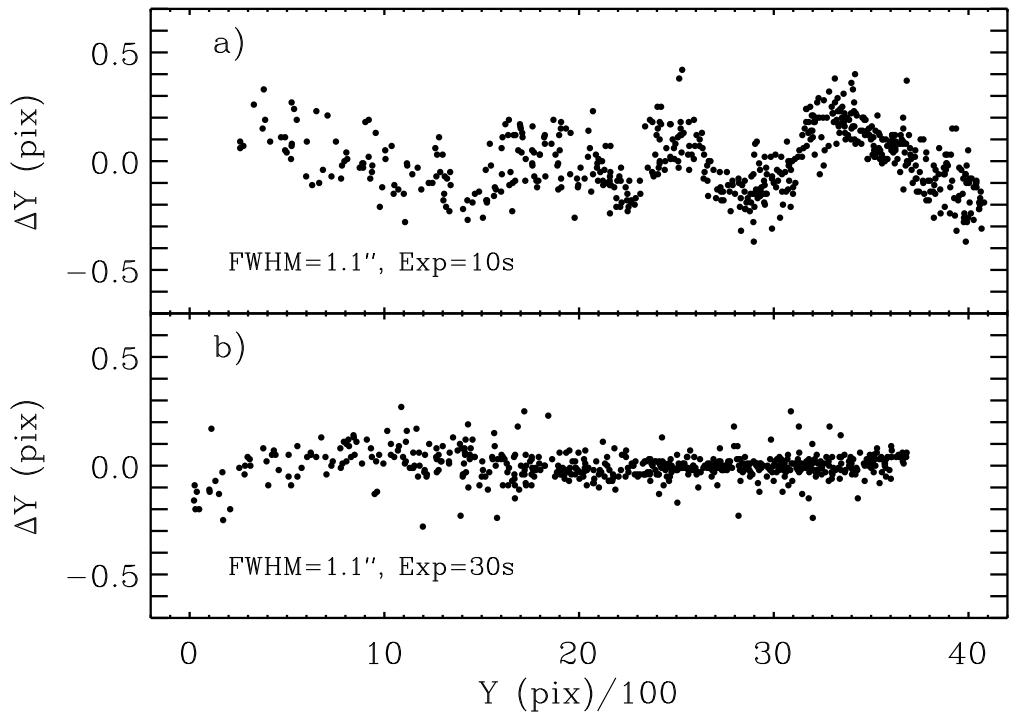

Fig. 9.— Coordinate differences in one NOAO CCD Mosaic Imager chip from two consecutive, slightly dithered, exposures. (a) The wiggles in the 10 s exposures are mostly due to atmospheric noise. (b) In the 30 s exposures the contribution of atmospheric noise is minimal. (Adapted from Platais et al. 2002.)

Table 1. First DAS fields

Field	RA[b]	Dec[b]	ℓ	b	λ	β	$E(B-V)$	$n_{\rm U}$[c]	$n_{\rm B}$[d]	$n_{\rm G}$[e]
GOT[a]	6:00	+21:45	187.8	−0.9	90.0	−1.7	1.4	2260	98K	192K
Hya	8:49	−15:25	241.2	+17.4	139.7	−31.9	0.1	1440	31K	28K
Oph	17:44	+11:15	35.6	+34.6	265.2	+34.6	0.2	1510	29K	22K
Sgr	19:20	−20:40	17.2	−15.3	288.7	+1.5	0.1	3720	360K	215K

[a]GOT stands for Gem-Ori-Tau, denoting the constellations covered in part.

[b]Equatorial coordinates (J2000) of the field center in hr, min for RA and in deg, arc-min for Dec; followed by Galactic, l and b, and ecliptic coordinates, λ and β, both in decimal deg.

[c]Number of UCAC2 stars per deg^2.

[d]Besançon model: predicted number of stars per deg^2 down to $V = 25$ (in thousands).

[e]Gilmore model: predicted number of stars per deg^2 down to $V = 25$ (in thousands).

Table 2. Suprime-Cam CCD chip constants

Chip	dx	dy	Θ	ϵ_{dx}	ϵ_{dy}	ϵ_{Θ}
0	-38.53	43.32	-0.004197	0.040	0.063	0.000023
1	39.46	38.82	-0.002558	0.022	0.046	0.000021
2	108.28	2.48	-0.002586	0.027	0.042	0.000015
3	186.38	-5.09	-0.002277	0.017	0.027	0.000025
4	194.42	29.84	-0.004793	0.020	0.043	0.000018
5	183.50	31.48	-0.003079	0.026	0.038	0.000010
6	17.64	9.41	-0.002141	0.011	0.060	0.000027
7	96.54	4.14	-0.002591	0.025	0.036	0.000021
8	330.08	-8.88	-0.003778	0.023	0.064	0.000020
9	271.17	24.30	-0.003386	0.043	0.064	0.000014